Structure of liquid caesium-bismuth alloys studied by neutron diffraction

van der Aart, S. A.; Verhoeven, V. W. J.; Verkerk, P.; van der Lugt, W.

Published in:
Journal of Chemical Physics

DOI:
10.1063/1.480612

Publication date:
2000

Structure of liquid caesium–bismuth alloys studied by neutron diffraction

S. A. van der Aart, V. W. J. Verhoeven, P. Verkerk, and W. van der Lugt

Citation: J. Chem. Phys. **112**, 857 (2000); doi: 10.1063/1.480612
View online: https://doi.org/10.1063/1.480612
View Table of Contents: http://aip.scitation.org/toc/jcp/112/2
Published by the American Institute of Physics

Structure of liquid caesium–bismuth alloys studied by neutron diffraction

S. A. van der Aart, V. W. J. Verhoeven, and P. Verkerk[a)]
Interfacultair Reactor Instituut, Delft University of Technology, 2629 JB Delft, The Netherlands

W. van der Lugt
Solid State Physics Laboratory, University of Groningen, 9747 AG Groningen, The Netherlands

(Received 3 August 1999; accepted 15 October 1999)

Neutron diffraction experiments were carried out for two liquid alloys with compositions CsBi and Cs_3Bi_2. The results indicate that probably polyanions with an average number of about two Bi atoms per cluster are formed. This result contrasts with that for liquid Cs–Sb, which contains larger chains as polyanions. © *2000 American Institute of Physics.* [S0021-9606(00)52102-3]

I. INTRODUCTION

In some respects the physical and chemical properties of the liquid Cs–Bi system are not well understood. The phase diagram[1] exhibits a deep eutectic at approximately 50% in between the congruently melting compounds Cs_3Bi and $CsBi_2$. The crystal structure of Cs_3Bi can be described as an NaTl lattice (two interpenetrating diamond lattices) with one-quarter of the lattice sites occupied by Bi.[2] Each Bi atom is in its first coordination shell completely surrounded by Cs atoms, in accordance with the electronegativity difference between the two components (1.23 on the Pauling scale). $CsBi_2$ forms a Laves ($MgCu_2$) structure.[2] The Bi atoms form a network of vertex-sharing tetrahedra; the bonding is not in accordance with the rules for Zintl phases.[3–5] Furthermore, there exists evidence for a compound Cs_3Bi_2 and a compound with approximate composition Cs_5Bi_4. The structure of neither of them could be determined.[6] Cs_3Bi_2 is peritectically melting, or nearly so. The phase diagram of the K–Bi[7] and Rb–Bi[8] systems are very similar to that of Cs–Bi.

From their relative positions in the Periodic Table one would expect a strong similarity between Bi and Sb and between their corresponding alloys. Indeed, such similarities are found for Tl and In and for Pb and Sn, which belong to the same two periods as Bi and Sb. In contrast, the physical and chemical properties of Bi and its alloys differ appreciably from those of Sb and its alloys.

In the phase diagrams of K–Sb, Rb–Sb, and Cs–Sb congruently melting equiatomic compounds occur.[9–11] The Sb ions in these compounds form tellurium-like infinite spiral chains in accordance with the rules for Zintl ion formation.[12,13] In the corresponding Bi systems these equiatomic compounds do not appear, but have given way to deep eutectics. There are strong indications that fragments of the Sb chains are preserved in the liquid state of the alkali–Sb alloys.[14,15] According to *ab initio* calculations the average length of a chain in liquid KSb is approximately five atoms.[15]

The resistivities of liquid Li–Bi alloys exhibit a distinct maximum at 25% Bi,[16] suggesting that the essentials of the crystal structure and the electronic structure of Li_3Bi are preserved in the liquid. In the sequence Li–Bi to Rb–Bi a second maximum at 40% Bi gradually appears, and for liquid Cs–Bi only the latter has survived.[17,18] In many cases of ionic alloys of alkali metals with post-transition polyvalent metals there is a strong relation between the crystal structure and the liquid structure.[4,19] In the case of Cs–Bi the resistivity data would indicate that the (unknown) structure of the compound Cs_3Bi_2 is somehow preserved in the liquid. There is, however, no trace of the Laves phase ($CsBi_2$) in the resistivity measurements. According to Tegze and Hafner[20] the solid Laves compounds are metallic due to a surplus of electrons, provided by the alkali atoms, on the otherwise covalent Bi network. Measurements of the Darken stability function of liquid Rb–Bi, which behaves very similar to Cs–Bi, suggest a compound at 50%, which is inconsistent with the resistivity measurements.[21] Cs–Sb exhibits a plateaulike maximum in the electrical resistivity between 35% and 50% Cs, which indicates that not only the Zintl compound CsSb plays a role in the liquid.[22] Tegze and Hafner[20] made a comprehensive theoretical investigation of the electronic structure of alkali-pnictide alloys. They attribute the difference between Sb and Bi alloys to the strong relativistic effects on the Bi orbitals.

Summarizing, the behavior of the Cs–Bi alloys is confusing, particularly around the eutectic composition. The present investigation constitutes an attempt to shed some light on the situation. Attention was focused on two compositions near the eutectic. Cs_3Bi_2 was chosen because there exists a solid compound of that composition, while CsBi was chosen for comparison with CsSb. As in this class of alloys, anion configurations (often Zintl ions) play an important role; neutron diffraction was chosen as the experimental technique. The occurrence of polyanions is often accompanied by a superstructure in the liquid, which shows up as a prepeak (''first sharp diffraction peak'') in the structure factor.

First, we describe experimental details. Next, the experimental data are analyzed by means of the reverse Monte Carlo (RMC) technique and with a scaling model.

a)Electronic mail: verkerk@iri.tudelft.nl

TABLE I. Composition of the Cs–Bi samples.

Sample	w_{Bi}(g)	w_{Cs}(g)	Composition (at. %)
Cs_3Bi_2	3.150	3.002	$Cs_{59.98}Bi_{40.02}$
CsBi	4.725	3.002	$Cs_{50.02}Bi_{49.98}$

II. EXPERIMENT

A. Samples

A cylindrical cell with a 0.6-mm-thick wall, 7 mm inner diameter, and 50 mm length was used. The cell is made of the alloy $Ti_{0.68}Zr_{0.32}$, which has zero coherent scattering length and produces completely incoherent background scattering without Bragg peaks. Furthermore, Ti–Zr is corrosion resistant against liquid alkali metals. However, the temperature should be kept below 800 °C, at which temperature the Ti–Zr alloy starts to soften and recrystallization can occur leading to Bragg peaks. Special care has to be taken to seal the cell leak tight, in particular at high temperatures. We use a knife edge and a screw lid to close the cell as described in Ref. 23. Because the knife edge is made of the same material as the cell there were no problems due to thermal expansion. The cell was tested and proved to be leak proof at high temperature.

The following metals were used for the preparation of the samples:

(a) Cs: vial 99.98%, Cabot (Revere, USA).
(b) Bi: ingots 99.999%, Ventron GmbH (Karlsruhe, Germany).

The samples were prepared in an argon-filled glovebox with O_2 and H_2O levels that are typically lower than 1 ppm.

Ti and Zr both have a poor resistance against liquid bismuth.[24] However, it is conceivable that the Cs–Bi mixture is less corrosive than the pure elements, because there is a strong compound formation. This is, for instance, indicated by the fast reaction between liquid Cs and solid Bi chunks. Unfortunately, no information on the corrosiveness of the Cs–Bi alloy is available. But after the measurements there were no indications for corrosion of the cell material.

Proper amounts of metal were transferred to the sample cell. After closing, the cell was heated up to 650 °C. Near the melting point of bismuth (271 °C) the heating was done very slowly in order to avoid a sudden fierce reaction which could destroy the cell. After measuring Cs_3Bi_2 the cell was opened in a glovebox and extra bismuth was added for the CsBi measurements. The cell was closed again with a new knife edge. The compositions of the samples are given in Table I.

B. Neutron diffraction

The experiments were performed on SLAD (Studsvik Liquids and Amorphous Materials Diffractometer) at the NFL (Neutronforskningslaboratoriet) in Studsvik, Sweden. SLAD has a medium resolution ($\Delta k/k \approx 0.01$) and a relatively high count rate. This resolution is sufficient in view of the broad features in the structure factor of a liquid material. As monochromator we used Cu (220) to select a wavelength of 0.11 nm. An oscillating collimator strongly reduced background scattering. There are four detector banks, each containing three Reuter–Stokes ^{3}He linear position-sensitive detectors with an active length of 60 cm. To cover the gaps between the four detector banks the detector box can rotate over 10°.

The angular range is $2° < 2\theta < 125°$, corresponding to an available range of momentum transfer $k = 4 - 93.6$ nm^{-1}. Each measurement was divided in several runs in order to check the stability of the system. The beam size was 3.5×1 cm^2.

During the measurements the reactor power varied from 37 MW during the empty can measurement to 47 MW during the sample and vanadium measurements. It turned out this was not well corrected for by the monitor in the incident beam, probably due to saturation of the monitor. The empty can measurement needed to be corrected for the difference in monitor efficiency at the respective reactor powers (3.6%).

The samples were measured at 550 °C. Cs_3Bi_2 was measured for 9 h in 13 runs, alternating the detector positions. This sample was heated up in the SLAD furnace where we could see from the diffraction pattern the bismuth melt at 271 °C, and immediately after that we saw new Bragg peaks appear at different positions. At around 440 °C these Bragg peaks disappeared. CsBi was measured for 11 h in 16 runs.

Corrections for attenuation, background, multiple scattering, and inelasticity (Placzek) were applied and the data were normalized by means of a vanadium measurement to an absolute value for the scattered intensity. The data corrections and normalization were performed using the program CORRECT, which is available at the NFL.[25]

After normalization, using first estimates of the unknown number densities ($\rho = 16.3$ nm^{-3} for Cs_3Bi_2, and $\rho = 17.8$ nm^{-3} for CsBi), the scattering level for large k turned out to be 0.453 b for Cs_3Bi_2 (using a filling fraction of the sample of 0.79 as estimated from x-ray photographs) and 0.481 b for CsBi (filling fraction of 0.94). The theoretically expected levels are 0.478 and 0.519 b, respectively. The difference is attributed to uncertainties in the density. The density has a noticeable effect only on the normalization, the effect on the multiple scattering correction is negligible. We therefore multiplied the data by a factor to obtain the theoretically expected scattering level, which is equivalent to choosing number densities of 15.4 and 16.5 nm^{-3} for Cs_3Bi_2 and CsBi, respectively.

The resulting experimental structure factors *S(k)* of Cs_3Bi_2 and CsBi at 550 °C are shown in Fig. 1. They show prepeaks at $k = 10.9$ and 10.7 nm^{-1}, respectively. Measurements on the Cs–Sb system by Lamparter, Martin, and Steeb[14] show that the prepeak remains at about the same position for CsSb and $Cs_{65}Sb_{35}$, namely 9.5 and 9.7 nm^{-1}, respectively. This contrasts with the Cs–Tl case,[26] where the prepeak increases in height and the position shifts to higher k with increasing Cs concentration.

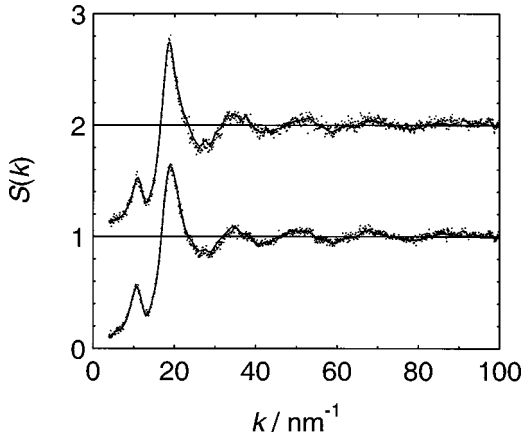

FIG. 1. Structure factors *S(k)* of liquid Cs_3Bi_2 (shifted vertically by +1) and CsBi at 550 °C. Dots: experimental results; solid line: MCGR fit.

TABLE II. Pair distances in crystalline alkali-Bi and alkaline earth–Bi alloys.

Pair	Alloy	Distance (nm)	Reference
Bi–Bi	$(cryptK^+)_2(Bi_4)^{2-}$	0.2936, 0.2941	28
	$Ca_{11}Bi_{10}$	0.315, 0.320	29
	$Ca_{14}MnBi_{11}$	0.3335	30
	$Sr_{14}MnBi_{11}$	0.3425	30
	$Ba_{14}MnBi_{11}$	0.3498	30
	KBi_2	0.335	31
	$CsBi_2$	0.345	2
	Cs_3Bi	0.658	2
Cs–Bi	Cs_3Bi	0.403	2
	$CsBi_2$	0.404	2
Cs–Cs	Cs_3Bi	0.403	2
	$CsBi_2$	0.423	2

III. ANALYSIS AND INTERPRETATION

A. Total pair distribution function and crystallographic data

By means of the program MCGR[27] we obtained from the experimental *S(k)* the total pair distribution functions defined by

$$g(r)=1+\frac{1}{2\pi^2\rho}\int_0^\infty k^2\{S(k)-1\}\frac{\sin kr}{kr}dr \tag{1a}$$

with the inverse:

$$S(k)=1+4\pi\rho\int_0^\infty r^2\{g(r)-1\}\frac{\sin kr}{kr}dr. \tag{1b}$$

By iteration using Eq. (1b) we fitted a smooth *g(r)* to the experimental data with the constraint that $g(r)\equiv 0$ for $r<0.26$ nm. The results for *S(k)* and *g(r)* are given in Figs. 1 and 2.

For the interpretation of *g(r)* it is useful to give some pair distances in crystalline alkali–Bi and alkaline earth–Bi alloys, see Table II. The largest distances for Bi–Bi and Cs–Cs (0.658 and 0.423 nm, respectively) are left out of consideration, because they most probably do not pertain to atoms in contact. Unfortunately, we could not find more data on Cs–Cs and Cs–Bi distances.

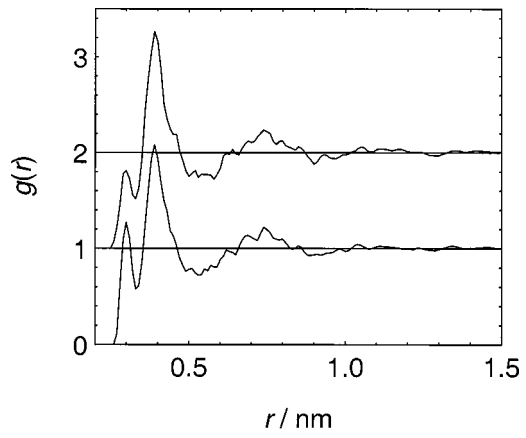

FIG. 2. Total pair distribution functions *g(r)* for liquid Cs_3Bi_2 (shifted vertically by +01) and CsBi at 550 °C, as obtained by Fourier transform of the experimental data by means of MCGR.

The total pair distribution functions of both Cs_3Bi_2 and CsBi exhibit distinct peaks at 0.30 and 0.39 nm (Fig. 2). The crystallographic data leaves us little choice for the first one: It should be attributed to Bi–Bi pairs. It is remarkable that the distance in the liquid is in the range of the shorter distances found in the solid. This indicates a strong covalent bond. The maximum of the second peak is situated very close to the Bi–Cs and Cs–Cs distances in the solid, but this peak is sufficiently broad to have appreciable values already at 0.35 nm. Therefore, it can, within the limits given by the crystallographic data, accommodate Bi–Bi pair distances as well.

B. RMC, partial structure factors

In order to obtain more insight we have estimated the partial pair distribution functions and partial structure factors by means of the reverse Monte Carlo method[32] (RMC). The differential cross section $d\sigma/d\Omega$ contains a weighted sum of the Faber–Ziman partial structure factors, $A_{\alpha\beta}(k)$:

$$\frac{1}{N}\frac{d\sigma}{d\Omega}=\sum_{\alpha,\beta} c_\alpha\overline{b_\alpha}c_\beta\overline{b_\beta}[A_{\alpha\beta}(k)-1]+\frac{\sigma_s}{4\pi}, \tag{2}$$

with c_α the concentration and $\overline{b_\alpha}$ the average coherent scattering length of component α, and σ_s the total scattering cross section of the alloy. The normalized weight factors $w_{\alpha\beta}=c_\alpha\overline{b_\alpha}c_\beta\overline{b_\beta}/\langle b\rangle^2$, with $\langle b\rangle=\Sigma_\alpha c_\alpha\overline{b_\alpha}$, are given in Table III. They are calculated using $\overline{b_{Cs}}=5.42$ fm and $\overline{b_{Bi}}=8.531$ fm.

TABLE III. Weight factors $w_{\alpha,\beta}$ for the partial structure factors $A_{\alpha,\beta}(q)$ and partial pair distribution functions $g_{\alpha,\beta}(r)$.

Alloy	$w_{Cs,Cs}$	$w_{Cs,Bi}$	$w_{Bi,Bi}$
Cs_3Bi_2	0.2381	0.4997	0.2622
CsBi	0.1509	0.4751	0.3740

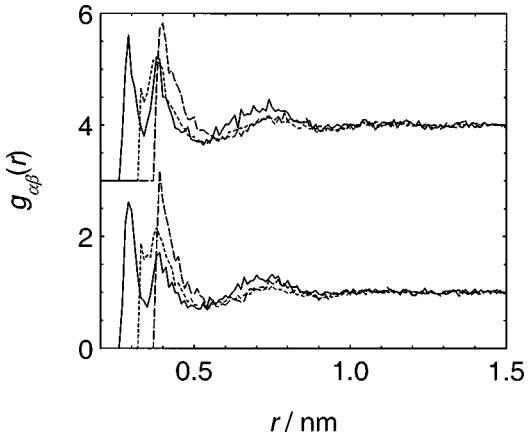

FIG. 3. The partial pair distribution functions $g_{\alpha\beta}(r)$ for Cs_3Bi_2 (shifted vertically by +3) and CsBi from RMC with cutoffs Cs–Cs:0.38, Cs–Bi: 0.325, Bi–Bi: 0.27 nm. Solid lines: $g_{\mathrm{Bi,Bi}}(r)$; short-dashed lines: $g_{\mathrm{Cs,Bi}}(r)$; long-dashed lines: $g_{\mathrm{Cs,Cs}}(r)$.

The number of particles was 3000 in both cases. The imposed number densities were 15.4 nm^{-3} for Cs_3Bi_2 and 16.5 nm^{-3} for CsBi. In the description of the results we will not distinguish between Cs_3Bi_2 and CsBi, as the general behavior of the two alloys is the same.

Unfortunately, the RMC results proved to be strongly dependent on the choice of the constraints imposed by the cutoff distances. Some tentative exercises with very relaxed constraints, viz. cutoff distances much smaller than the nearest-neighbor distances found in the crystals, did not result in well-separated partial structure factors.

The constraints were then tightened by choosing 0.27 nm for Bi–Bi and 0.38 nm for Bi–Cs and Cs–Cs, all 0.02 nm shorter than the corresponding nearest-neighbor distances in the solid (see Table II). This choice resulted in a good resolution of the partials, but also created problems at low k: The partial structure factors for Bi–Bi and Cs–Cs diverged for k approaching zero. In addition large wiggles developed below 15 nm^{-1}. The diverging behavior becomes even stronger when the number of particles is increased to 6000. This strongly suggests phase separation in the RMC configuration, which makes these constraints physically unacceptable. Prepeaks at 10 nm^{-1} can be discerned in the Bi–Bi partials, although they are partly masked by the wiggles.

It is curious that the Bi–Cs distance found in crystalline Cs_3Bi_2 is equal to the Cs–Cs distance and much larger than the Bi–Bi distances found in various crystals. This is probably enforced by the particular cubic crystal structures. The lack of crystallographic data on Cs–Bi distances is particularly troublesome here. We therefore replaced the Cs–Bi distance by 0.325 nm, which is the average of the Cs–Cs and Bi–Bi cutoff distances. Now at small k the partial structure factors fall off much more smoothly to decently low values. The Bi–Bi partial structure factors (not shown in the figures) display distinct prepeaks at 10 nm^{-1}, whereas no prepeaks are visible in the other partial structure factors. This last set of cutoff distances was adopted for further computations. Evidently the Bi–Bi correlations are responsible for the prepeak and, consequently, for the long-range order in the liquid.

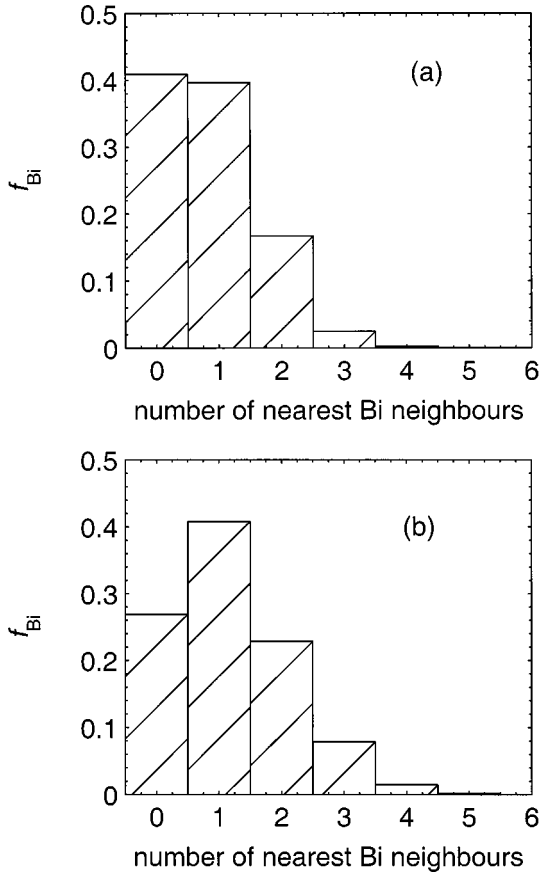

FIG. 4. Distribution f_{Bi} of Bi–Bi coordination numbers within 0.340 nm from the central Bi atom. (a) Cs_3Bi_2, (b) CsBi.

The total structure factors fitted to the experimental data by RMC are not given separately, because they virtually coincide with the MCGR structure factors in Fig. 1.

C. Partial pair distribution functions

Figure 3 shows the partial pair distribution functions $g_{\alpha\beta}(r)$ for the set of cutoff distances finally adopted. We find Bi–Bi peaks at 0.29 and 0.38 nm. The main Cs–Bi peak occurs at 0.38 nm, but has still appreciable values at 0.35 nm, and the Cs–Cs peak occurs at 0.39 nm. The most interesting feature is the Bi–Bi peak at 0.29 nm. It suggests the presence of Bi clusters with remarkably short bond length.

The position of the first peak in $g_{\mathrm{Bi,Bi}}(r)$ should be compared to the known Bi–Bi distances in crystalline alkali–Bi and alkaline earth–Bi alloys, as given in Table II. The Bi–Bi distance of 0.29 nm corresponds to the shortest value found in crystalline materials. This indicates a strongly covalent bond. It is therefore interesting to estimate the Bi–Bi coordination number. We have calculated this number from the RMC configurations for a maximum Bi–Bi distance of 0.340 nm. The distribution of the Bi–Bi coordination numbers is given in Fig. 4. The average numbers are 0.815 for Cs_3Bi_2 and 1.17 for CsBi.

The Bi–Bi–Bi bond angle distributions are given in Fig. 5. There is a peak at $\cos\varphi = 0.12$, corresponding to $\varphi = 83°$,

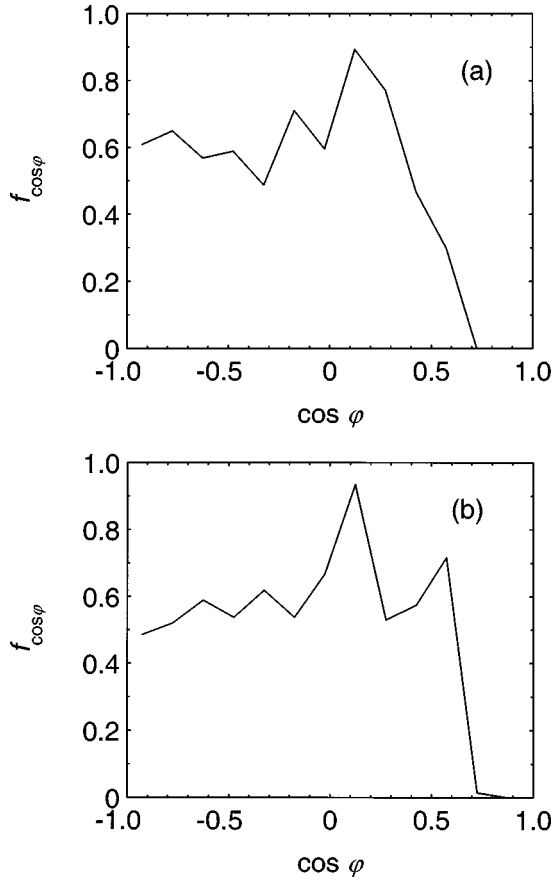

FIG. 5. Bi–Bi–Bi bond angle distribution $f_{\cos\varphi}$ for a maximum Bi–Bi bond of 0.340 nm. (a) Cs_3Bi_2. (b) CsBi.

which is close to the angle of 90° found in Bi_4^{2-} units and in the Sb chains in the alkali–Sb alloys.

D. Scaling model

The three-dimensional model fitted to the experimental data by means of RMC indicates that the prepeak is due to the arrangement of the Bi atoms and that the Bi–Bi distance is in the range of the shorter distances found in crystalline materials. It therefore makes sense to describe the structure in terms of a cluster model. In order to obtain information on the size of the clusters we use a scaling model that has been described previously.[19,26] It is based on the trivial fact that, if the bismuth atoms form part of clusters of n Bi atoms, the number density of clusters is equal to the number density of single bismuth atoms divided by n. Then the average intercluster distance scales approximately with $n^{1/3}$, all at constant total volume.

This is made quantitative by putting the clusters on an imaginative fcc lattice. We can then define a sort of Wigner–Seitz (or Voronoi) cell around every cluster and calculate the volume of the cell, Ω_{cell}, and the number of atoms of the two species (Bi and Cs in this case) in it. Finally the intercluster distance d is related to the prepeak position, k_0, by

$$k_0 d = 7.7. \tag{3}$$

Thus we find

$$d = 2^{1/6}\Omega_{\text{cell}}^{1/3}, \tag{4}$$

$$\Omega_{\text{cell}} = \frac{1}{\sqrt{2}}\left(\frac{7.7}{k_0}\right)^3, \tag{5}$$

and

$$N_i = c_i \rho \frac{1}{\sqrt{2}}\left(\frac{7.7}{k_0}\right)^3, \tag{6}$$

where N_i is the number of atoms of the species i in the unit cell, c_i is their fraction, and ρ is the total number density of atoms.

Substitution of $k_0 = 10.9$ nm^{-1}, $\rho = 15.4$ nm^{-3}, and $k_0 = 10.7$ nm^{-3}, $\rho = 16.5$ nm^{-3} for Cs_3Bi_2 and CsBi, respectively (see the following for the method of estimating the densities) we find that the number of Bi atoms in a cell is 1.54 in Cs_3Bi_2 and 2.17 in CsBi. These numbers are consistent with the independently determined average coordination numbers 0.815 for Cs_3Bi_2 and 1.17 for CsBi. This confirms the trend found in the solid alloys that Bi atoms in alkali–bismuth alloys have only little tendency to form large Zintl ions. For comparison: in liquid KSb the average number of atoms in the Sb chain fragments is approximately 5 according to the *ab initio* calculations by Seifert-Lorenz and Hafner.[15] In the Bi alloys dumbbells appear to predominate.

At this point, a critical evaluation of the validity of the model and of the accuracy of the numbers given above is due. The ''scaling model'' is built up in several steps, each of them introducing an error. First, the relation $k_0 d = 7.7$ is based on the simplification that the prepeak is a delta function. In that approximation the number 7.7 is the value of kd for which $\langle \exp(\mathbf{k}\cdot\mathbf{d})\rangle_{\text{spherical}}$ has its first nontrivial maximum. This maximum, however, is broad, approximately similar to the maxima of a sine function. The influence of the final width of the prepeak is not easy to assess but some computational exercises show that the value of kd might vary between 7.3 and 7.9. Moreover, the relation has been widely confirmed empirically[19] for other systems.

Second, the choice of a fcc lattice is somewhat arbitrary, though its high symmetry makes it a good substitute for the spherical symmetry of the liquid. On the other hand the liquid is not likely to have the optimum packing of the fcc lattice, as neither the contents of the ''cells'' are identical, nor the ''lattice vectors'' are all equal in length. The worst packing we can reasonably imagine as a substitute is simple cubic. In that case the factors $\sqrt{2}$ in the denominators of Eqs. (5) and (6) disappear, and consequently the values of N_i would become higher by 41%.

The third source of errors are the liquid densities. They have not been measured directly, but estimates have been obtained indirectly from the normalization procedure (see Sec. II). They can also be estimated starting from the known densities of solid Cs_3Bi and $CsBi_2$. Then there remain two major problems: to account for the enormous volume contraction (48% for Cs_3Bi and 38% for $CsBi_2$ in the solid state) and for the volume change on melting and heating. The volume contraction is a chemical effect: it is largely a consequence of the large caesium atoms being deprived of their s electrons. We assume that the corresponding change in

atomic volume in the liquid state is equal to that in the solid state. The latter was obtained by linear interpolation between the values for Cs_3Bi and $CsBi_2$. Furthermore, we have assumed that the effects of thermal expansion and chemical volume contraction are mutually independent. Therefore, we simply linearly interpolated the ideal liquid atomic volumes between those for pure Cs and pure Bi and corrected them for the atomic volume changes due to the chemical contraction. The estimated atomic volumes are then 0.0614 nm^3 for Cs_3Bi_2 and 0.0560 nm^3 for CsBi, corresponding to total number densities of 16.3 and 17.8 nm^{-3}. These values are in fair agreement with the values obtained from the normalization (15.4 and 16.5 nm^{-3}, respectively). As sources for the densities we have used Ref. 2 (solid alloys), and Refs. 33–35 (solid and liquid pure metals). We have decided, somewhat arbitrarily, to adopt the values found from the normalization, with an estimated error of $\pm 15\%$.

Summing up, another choice of the cubic lattice may push N_i in an upward direction while the other possible errors are random. Combining the error estimates we think that for Cs_3Bi_2 $N_{Bi}=1.5$ with lower and upper error limits of 1.2 and 2.3 and that for CsBi $N_{Bi}=2.2$ with lower and upper limits of 1.8 and 3.0. These numbers are fairly consistent with the estimates for the Bi–Bi coordination obtained from the RMC analysis. Our conclusion that the clusters are considerably smaller than in the corresponding Sb alloys seems justified. The occurrence of Bi_2 dimers is nicely illustrated in Fig. 6, which displays part of the RMC generated configurations of Cs_3Bi_2 and CsBi. Bonds are drawn for Bi–Bi distances <0.340 nm.

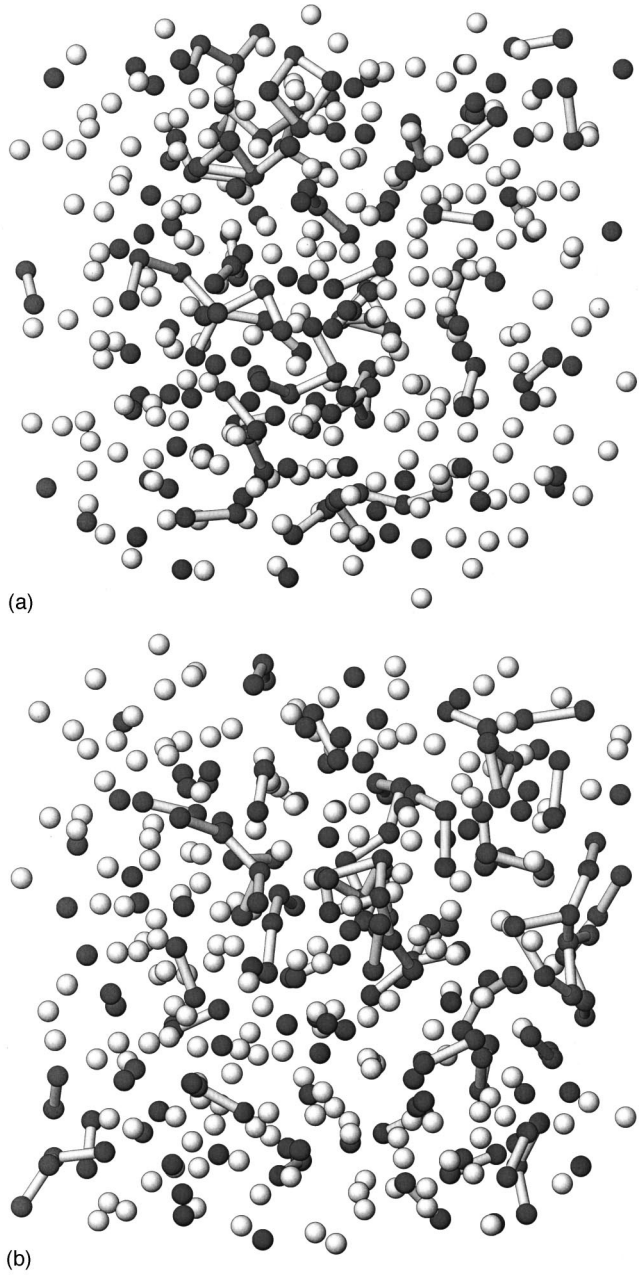

FIG. 6. Part (1/8) of the RMC configurations for liquid (a) Cs_3Bi_2 and (b) CsBi. White particles: Cs; gray particles: Bi. The bonds indicate Bi–Bi distances <0.340 nm.

IV. CONCLUSION

The neutron diffraction patterns of liquid Cs_3Bi_2 and CsBi alloys exhibit a pronounced prepeak indicating a superstructure. RMC analysis and comparison with crystallographic data shows that the superstructure is due to the arrangement of the Bi atoms, that the Bi–Bi distance corresponds to the shortest distances found in the solid, and that the average coordination numbers are 0.815 and 1.17, respectively. The Bi–Bi–Bi bond angle distribution has a maximum near 90°, the angle found in Bi_4^{2-} units.

According to the scaling model the average number of Bi atoms participating in a cluster is 1.54 for Cs_3Bi_2 and 2.17 for CsBi. All the data support the supposition that small, strongly covalent clusters occur in the liquid, many of them in the form of dimers Bi_2^{2-}, but single Bi ions and small chains are also present. In this respect the Cs–Bi alloys differ strongly from their Cs–Sb counterparts. Bi_2^{2-} units have also been found in gas-phase Zintl ions $(Ba_2Na)^{3+}$.[36] They are isoelectronic to the neutral Te_2 clusters.[37,38]

The results suggest that there is a gradual transition from the octet compound Cs_3Bi to the Laves compound $CsBi_2$. In the first one the Bi atoms occur isolated. For higher Bi concentrations small Bi clusters develop, which grow in size as more bismuth is added until ultimately the network typical for the Laves compound is formed. Such a gradual transition is evidently accommodated by the liquid more easily than by the solid state. This would explain the occurrence of a deep eutectic.

Our findings are in agreement with the conclusions of Tegze and Hafner[20] that the chain structure as occurring in CsSb is destabilized because of the more extended nature of the Bi 6*p* orbitals. Obviously, a structure with small clusters is preferred.

Quite recently, Xu and Sevov[39] informed us that they had found Bi–Bi distances as short as 0.2838 nm in $(K\text{-crypt})_2Bi_2$, which they explained by assuming a double bond between the bismuth atoms. This is in remarkably good agreement with the short bond length (0.29 nm) found in the liquid. A similar isolated Bi dumbbell with a bond length of

0.3113 nm has recently been found in KBa_4Bi_3O by the group of Eisenmann.[40]

ACKNOWLEDGMENTS

We acknowledge financial support from the EC Large Scale Facilities programme. The staff of NFL is thanked for support during the measurements. This work has benefitted from fruitful discussions with Professor Eisenmann from the Eduard-Zintl-Institut, Darmstadt.

[1] J. Sangster and A. D. Pelton, J. Phase Equilib. **12**, 443 (1991).
[2] G. Gnutzmann, F. W. Dorn, and W. Klemm, Z. Anorg. Allg. Chem. **309**, 210 (1961).
[3] W. Klemm and E. Busmann, Z. Anorg. Allg. Chem. **216**, 195 (1932).
[4] *Chemistry, Structure and Bonding of Zintl Phases and Ions*, edited by S. Kauzlarich (VCH, New York, 1996).
[5] R. Nesper, Prog. Solid State Chem. **20**, 1 (1990).
[6] G. Gnutzman and W. Klemm, Z. Anorg. Allg. Chem. **309**, 181 (1961).
[7] A. Petric and A. D. Pelton, J. Phase Equilib. **12**, 29 (1991).
[8] A. D. Pelton and A. Petric, J. Phase Equilib. **14**, 368 (1993).
[9] J. Sangster and A. D. Pelton, J. Phase Equilib. **14**, 510 (1993).
[10] J. Sangster and A. D. Pelton, J. Phase Equilib. **18**, 390 (1997).
[11] J. Sangster and A. D. Pelton, J. Phase Equilib. **18**, 382 (1997).
[12] H. G. von Schnering, W. Hönle, and G. Krogull, Z. Naturforsch. B **34**, 1678 (1979).
[13] E. Busmann and S. Lohmeyer, Z. Anorg. Allg. Chem. **312**, 53 (1961).
[14] P. Lamparter, W. Martin, and S. Steeb, Z. Naturforsch. A **38**, 329 (1983).
[15] K. Seifert-Lorenz and J. Hafner, Phys. Rev. B **59**, 843 (1999).
[16] G. Steinleitner, W. Freyland, and F. Hensel, Ber. Bunsenges. Phys. Chem. **79**, 1186 (1975).
[17] J. A. Meijer and W. van der Lugt, J. Phys.: Condens. Matter **1**, 9779 (1989).
[18] R. Xu, R. Kinderman, and W. van der Lugt, J. Phys.: Condens. Matter **3**, 127 (1991).
[19] W. van der Lugt, J. Phys.: Condens. Matter **8**, 6115 (1996).
[20] M. Tegze and J. Hafner, J. Phys.: Condens. Matter **4**, 2449 (1992).
[21] J. J. Egan, High Temp. Science **19**, 111 (1985).
[22] J. Bernard and W. Freyland, J. Non-Cryst. Solids **205–207**, 62 (1996).
[23] P. Verkerk, Nucl. Instrum. Methods **160**, 19 (1980).
[24] *The Liquid Metals Handbook*, 2nd ed., edited by R. N. Lyon and D. L. Katz (USGPO, Washington, DC, 1954).
[25] M. A. Howe and R. L. McGreevy, CORRECT: A correction programme for neutron diffraction data, version 2.18, April 1995.
[26] S. A. van der Aart, P. Verkerk, Y. S. Badyal, and W. van der Lugt, J. Chem. Phys. **108**, 9214 (1998).
[27] Electronic mail: http://www.studsvik.uu.se/rmc/rmchome.htm
[28] A. Cisar and J. D. Corbett, Inorg. Chem. **16**, 2482 (1977).
[29] K. Deller and B. Eisenmann, Z. Naturforsch. B **31**, 29 (1975).
[30] T. Y. Kuromoto, S. M. Kauzlarich, and D. J. Webb, Chem. Mater. **4**, 435 (1992); S. M. Kauzlarich in Ref. 4, p. 245.
[31] E. Zintl and A. Harder, Z. Phys. Chem. Abt. B **16**, 206 (1932).
[32] R. L. McGreevy and L. Pusztai, Mol. Simul. **1**, 359 (1988).
[33] T. Iida and R. I. L. Guthrie, *The Physical Properties of Liquid Metals* (Clarendon, Oxford, 1988).
[34] *Handbook of Thermodynamic and Transport Properties of Alkali Metals*, edited by R. W. Ohse (Blackwell, Oxford, 1985).
[35] *Handbook of Chemistry and Physics*, 53rd ed. (Chemical Rubber, Cleveland, OH, 1972).
[36] R. W. Farley and A. W. Castleman, Jr., J. Am. Chem. Soc. **111**, 2734 (1989).
[37] G. Igel-Mann, H. Stoll, and H. Preuss, Mol. Phys. **80**, 341 (1993).
[38] C. Heinemann, W. Koch, and P.-O. Widmark, Mol. Phys. **92**, 463 (1997).
[39] L. Xu and S. C. Sevov (private communication).
[40] B. Eisenmann (private communication).